Use of CONTIN for Calculation of Adsorption Energy Distribution †

ARTICLE *in* LANGMUIR · APRIL 1999

Impact Factor: 4.46 · DOI: 10.1021/la981369t

4 AUTHORS, INCLUDING:

Alexander M. Puziy
National Academy of Sciences of Ukraine
80 PUBLICATIONS **1,534** CITATIONS

Use of CONTIN for Calculation of Adsorption Energy Distribution†

A. M. Puziy,*,‡ T. Matynia,§ B. Gawdzik,§ and O. I. Poddubnaya‡

Institute for Sorption and Problems of Endoecology, Naumov St. 13, 252164 Kiev, Ukraine, and MCS University, Faculty of Chemistry, Pl. Marii Curie-Sklodowskiej 3, 20031 Lublin, Poland

Received October 2, 1998. In Final Form: February 4, 1999

The CONTIN method for inverting noisy linear operators was used to calculate the adsorption distribution function from both simulated and experimental adsorption isotherms. Simulated isotherms allowed us to estimate the resolving power of the method and the influence of errors on the distribution function, while experimental isotherms enabled us to validate the adsorption model and its parameters. It was shown that calculation within the condensation approximation region gives perfect recovering of the original distribution if sufficient information is inherent in the input data, that is, in the case of a large data set over a wide range of relative pressures. When only a window of data is available on the adsorption isotherm, it is possible to calculate the distribution restricted to the condensation approximation (CA) region. The influence of peaks outside the CA region may be eliminated by introducing the constant background term in the calculation. The level of error on the isotherm does not affect the resulting distribution up to 10% in the case of a large data set and up to 5% in the case of a small data set. On the basis of analysis of the randomness of the residuals of the fit to the data, it was possible to establish a true parameter of the lateral interaction constant. This approach applied to experimental data has led to the value $k_1^{mob} = 5.5-5.6$ for the HdB mobile adsorption model and $k_1^{loc} = 3$ for the FG localized adsorption model. On the basis of the fact that optimal value of k_1^{mob} is closer to the theoretical value, the mobile adsorption model is preferred. The CONTIN method applied to graphitized carbon black revealed four peaks on the adsorption energy distribution function. The peak constrained analysis allowed us to confirm the existence of all original peaks. The distributions calculated from standard nitrogen adsorption data showed that although reference carbons are heterogeneous in different ways, they possess common peaks at 4.9, 6.8, and 8.8 kJ/mol characteristic to graphitized carbon black Sterling FT. Analysis of the heterogeneity of synthetic carbons revealed the changes in adsorption energy distributions (AEDs) that occur during CVD from methane.

1. Introduction

Analysis of physical adsorption data has become a standard method for assessment of the heterogeneity of solid adsorbents. The theoretical description of adsorption on heterogeneous adsorbents is almost exclusively interpreted by superposition of adsorption on independent homogeneous sorption sites. This concept leads to a Fredholm integral equation of the first kind:

$$\Theta_t(p) = \int_{U_{min}}^{U_{max}} \Theta_t(p,U)\, f(U)\, dU \qquad (1)$$

where the desired distribution function *f(U)*, is to be estimated from experimental adsorption data, Θ_t, of limited accuracy. The kernel function $\Theta_l(p,U)$ (local isotherm) describes adsorption on a homogeneous site characterized by property *U* (energy, pore size, etc.). Since the distribution function is widely used for characterization of adsorbents, many methods have been developed for calculating the distribution function from adsorption data. A comprehensive review of the methods for assessment of the adsorption energy distribution may be found elsewhere.[1−3] Estimating the distribution function from eq 1 is a well-known ill-posed problem, which is manifested by the fact that there exists an infinitely large set of possible solutions, all satisfying eq 1 to within the experimental errors. In other words, all solutions may have arbitrary large deviations from each other and from the true solution and yet equally well fit the experimental data. To select the meaningful solution from the set of all possible solutions, two main routes are commonly used (Figure 1). In first group, local isotherm approximation (LIA) methods, the local isotherm is approximated by a simple function, which makes it possible to solve eq 1 analytically for the distribution function.[4] The best known example for LIA methods is the condensation approximation (CA) with approximation of the local isotherm by a step function. A general framework for methods related to local isotherm approximations may be found elsewhere.[9] The LIA family gives a reasonably good solution for smooth distributions. An important advantage of the LIA meth-

† Presented at the Third International Symposium on Effects of Surface Heterogeneity in Adsorption and Catalysis on Solids, held in Poland, August 9−16, 1998.

* Corresponding author. E-mail: alexander.puziy@ispe.kiev.ua. Fax: (38-044) 452-9327.

‡ Institute for Sorption and Problems of Endoecology.

§ MCS University.

(1) Jaroniec, M.; Madey, R. *Physical Adsorption on Heterogeneous Solids*; Elsevier: Amsterdam, 1988.

(2) Rudzinski, W.; Everett, D. H. *Adsorption of Gases on Heterogeneous Surfaces*; Academic Press: New York, 1992.

(3) Cerofolini, G. F.; Re, N. *Riv. Nuovo Cimento Soc. Ital. Fis.* **1993**, *16*, 1.

(4) Roginski, S. S. *Adsorption and Catalysis on Heterogeneous Surfaces*; Academy of Sciences of USSR: Moscow, 1948.

(5) Harris, L. B. *Surf. Sci.* **1968**, *10*, 129.

(6) Cerofolini, G. F. *Surf. Sci.* **1971**, *24*, 391.

(7) Cerofolini, G. F. *Thin Solid Films* **1974**, *23*, 129.

(8) Nederlof, M. M.; Van Riemsdijk, W. H.; Koopal, L. K. *Environ. Sci. Technol.* **1992**, *26*, 763.

(9) Nederlof, M. M.; Van Riemsdijk, W. H.; Koopal, L. K. *J. Colloid Interface Sci.* **1990**, *135*, 410.

(10) Rudzinski, W.; Jagiello, J.; Grillet, Y. *J. Colloid Interface Sci.* **1982**, *87*, 478.

(11) Jagiello, J.; Ligner, G.; Papirer, E. *J. Colloid Interface Sci.* **1989**, *137*, 128.

10.1021/la981369t CCC: $18.00
Published on Web 04/22/1999

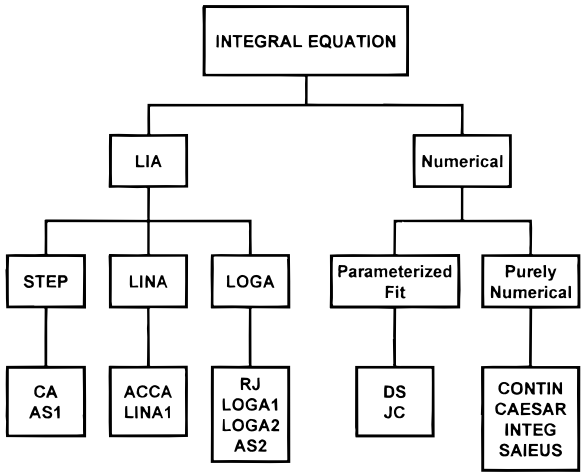

Figure 1. Diagram of methods used for the solution of the adsorption integral equation.

odology is that it is applicable when only a window of data is available. Alternatively, more rigorous are numerical methods which addresses the ill-posedness of eq 1 explicitly.[12−17] Numerical methods deserve more attention due to their potential accuracy and higher resolving power over the LIA methods.[18] The major problems in application of numerical methods are connected with the choice of local isotherm and stabilization of the solution. While a suitable kernel for eq 1 is based on physical insight on the adsorption process and can be obtained from analysis of adsorption on a homogeneous adsorbent, the choice of stabilization parameter is not known beforehand. A simple strategy for stabilizing an ill-posed problem is to reduce the number of degrees of freedom by fitting a parametrized solution to the data. The well-known Dubinin−Stoeckli equation with Gauss distribution and the Jaroniec−Choma equation with Gamma distribution are examples of this method. Although this approach is widely used, the correct number of degrees of freedom is usually very difficult to specify a priori. As a result, this approach almost always gives a biased, distorted solution. Another common strategy for stabilizing the solution is purely numerical solution of eq 1. These methods have been reviewed and closely examined in refs 12−14. We will briefly mention only several of them: CAESAR—computed adsorption energies using singular value decomposition,[13,19,20] INTEG—solution of adsorption integral equations,[12] SAIEUS—solution of adsorption integral equations using splines.[14] There exists, however, another mature method for inverting noisy linear operators—CONTIN, developed by Provencher.[16,17] Despite the fact that the underlying mathematics of this method have been well worked out and its efficiency has been shown in the field of physical sciences, it still has not been applied to adsorption problems. The purpose of this paper is to demonstrate the efficiency of the CONTIN method for solution of adsorption integral in eq 1 with respect to the adsorption energy distribution (AED). CONTIN is a general purpose constrained regularization method which finds the simplest (most parsimonious) solution that is consistent with prior knowledge and the experimental data. Numerically stable orthogonal decomposition and quadratic programming algorithms are used to obtain the unique global solution subject to any linear equality or inequality constraints imposed by prior knowledge (e.g. nonnegativity). CONTIN has several favorable features. The first advantage of this method is the automatic choice of the regularization parameter on the basis of an F-test and confidence regions and thus it provides an optimal solution in an objective way. However, CONTIN outputs all solutions so the user is able to check the fit using other prior knowledge. A second advantage of the CONTIN method is that it allows one to introduce a constant background term in the calculation and thus consider explicitly the influence of adsorption sites having energy far beyond the region where the distribution function is calculated. This is an important option because most of the experimental data contain only part of the overall isotherm. Thus, the distribution function can be calculated only over the experimentally measured region avoiding the influence of adsorption sites which cannot be reliably calculated. The third advantage is extensive analysis of errors of the fit to the data. This can help to validate the adsorption model and choose its optimal parameters. Furthermore, a peak-constrained analysis provided by CONTIN is helpful for revealing the artifacts on the calculated distribution. And finally, the flexibility of the program merits notice: CONTIN is written in FORTRAN and can easily be changed to fit any specific problem. The source code for CONTIN is available via the Internet at http://www.provencher.de.

To test CONTIN calculating the adsorption energy distribution function, both simulated and experimental isotherms were used. Analysis of simulated isotherms provides a means for estimating the influence of errors, measured pressure range, and quantity of available data points in the isotherm on the resulting distribution function, while analysis of experimental isotherms makes possible testing the validity of the adsorption model and helps us to establish optimal parameters. A more accepted adsorption model will be used for characterizing the heterogeneity of carbonaceous adsorbents.

Table 1. Characteristics of Simulated Isotherms

set	N	$P/P_{0\ min}$	$PP_{0\ max}$	U_{min}, kJ/mol	U_{max}, kJ/mol	error, %
1	50	10^{-5}	0.1	5.06	10.95	0−10
2	50	10^{-3}	0.1	5.06	8.01	0−10
3	10	10^{-5}	0.1	5.06	10.95	0−10
4	10	10^{-3}	0.1	5.06	8.01	0−10

2. Experimental Section

2.1. Isotherms. *2.1.1. Simulated Isotherms.* Simulated isotherms were calculated equally spaced along the P/P_0 range using the HdB equation as local isotherm and a four-peak Gaussian distribution function with the following parameters: $w_i = 0.25$; $U_{0i} = 6$, 7.5, 9, and 10.5; and $\sigma_i = 0.25$. After calculation the random relative error with levels 0, 1, 5, and 10% was imposed on the adsorption value. There was no error imposed on the P/P_0 value. Table 1 lists characteristic features of simulated isotherms: N, the number of experimental points on the isotherm, the relative pressure range and corresponding energy range calculated using the condensation approximation (CA), and the error imposed on the isotherm. Four different data sets have been calculated to represent various experimental conditions. The first data set is characterized by a sufficiently large number of experimental points ($N = 50$) on the isotherm and a wide range of relative pressure $P/P_0 = 10^{-5}$ to 0.1. The chosen relative

(12) Von Szombathely, M.; Braüer, P.; Jaroniec, M. *J. Comput. Chem.* **1992**, *13*, 17.
(13) Koopal, L. K.; Vos, C. H. W. *Langmuir* **1993**, *9*, 2593.
(14) Jagiello, J. *Langmuir* **1994**, *10*, 2778.
(15) Puziy, A. M.; Volkov, V. V.; Poznayeva, O. I.; Bogillo, V. I.; Shkilev, V. P. *Langmuir* **1997**, *13*, 1303.
(16) Provencher, S. W. *Comput. Phys. Commun.* **1982**, *27*, 213.
(17) Provencher, S. W. *Comput. Phys. Commun.* **1982**, *27*, 229.
(18) Jagiello, J.; Bandosz, T. J.; Schwarz, J. A. *Carbon* **1994**, *32*, 1026.
(19) Koopal, L. K.; Vos, K. H. W. *Colloid Surf.* **1985**, *14*, 87.
(20) Vos, K. H. W.; Koopal, L. K. *J. Colloid Interface Sci.* **1985**, *105*, 183.

Table 2. Characteristics of Experimental Isotherms

carbon	ref	N	$P/P_{0\ min}$	$P/P_{0\ max}$	U_{min}, kJ/mol	U_{max}, kJ/mol
Sterling FT 2800	21	28	3×10^{-5}	0.1	5.06	10.25
Vulcan	22	19	3×10^{-4}	0.1053	5.02	8.78
Carbon A	23	10	5×10^{-3}	0.1	5.06	6.98
Standard	24	12	5×10^{-3}	0.1	5.06	6.98
NPC	25	38	3×10^{-5}	0.1	5.06	9.92
BM-ST	26	8	1.31×10^{-2}	0.351	4.25	6.36
C1	26	12	2.0×10^{-5}	0.379	4.20	10.51
C2	26	10	9.3×10^{-3}	0.200	4.61	6.58
C3	26	10	1.14×10^{-2}	0.200	4.61	6.45

pressure range is sufficiently wide to cover all peaks of the original distribution function. The second data set was calculated for a sufficiently large number of experimental points ($N = 50$) but over higher relative pressures ($P/P_0 = 10^{-3}$ to 0.1). The third data set was calculated for a small number of experimental points ($N = 10$) over a wide range of relative pressure ($P/P_0 = 10^{-5}$ to 0.1). And the fourth data set corresponding to poor-quality experimental data possesses a small number of experimental points ($N = 10$) calculated for high relative pressures ($P/P_0 = 10^{-3}$ to 0.1).

2.1.2. Experimental Isotherms. In the present work several experimental nitrogen adsorption isotherms on carbon adsorbents have been used (Table 2). The first is nitrogen adsorption on a classical homogeneous carbon adsorbent—carbon black Sterling FT 2800 graphitized at 3000 ± 300 °C in the absence of air.[21] It was also of interest to estimate the heterogeneity of reference carbon adsorbents which are widely used in the α_s method. In the present study the following standard isotherms have been analyzed: the nitrogen adsorption isotherm on untreated Vulcan carbon black,[22] the standard nitrogen adsorption isotherm on carbon A,[23] the standard nitrogen adsorption data for nonporous carbon,[24] and the standard data of nitrogen adsorption on nonporous carbon black NPC.[25] To avoid the multilayer adsorption region, only part of the isotherms with points below $P/P_0 = 0.1$ was used for calculation.

Nitrogen adsorption isotherms on synthetic carbons obtained from the porous polyimide copolymer BM-ST[26] were also used for analysis of changes in the AED under various carbonization procedures. Carbon C1 was obtained by carbonization of the parent BM-ST copolymer to 600 °C with the heating rate 10 °/min in a nitrogen atmosphere. Carbon C2 was obtained by heat treatment of sample C1 in an atmosphere of CH_4 at 900 °C for 1 h. Carbon C3 was obtained by a two-step carbonization of the parent BM-ST copolymer. The first step was oxidative stabilization at 300 °C for 1 h in air, and the second step comprised carbonization in an atmosphere of CH_4 up to 900 °C with the heating rate 10°/min. Nitrogen adsorption isotherms were measured at 77 K by using a ASAP 2010 (Micromeritics, Norcross, GA) volumetric sorption analyzer. Before adsorption measurements samples were outgassed under vacuum at 200 °C, except copolymer BM-ST, which was heated to 120 °C.

2.2. Calculation Method. For the purpose of the present work two model adsorption equations were introduced into the CONTIN program. The first is a mobile adsorption model with the Hill−de Boer equation:

$$P = \frac{\Theta}{1-\Theta} K_0^{\ mob} \exp\left(-\frac{U}{RT} - k_1^{mob}\Theta + \frac{\Theta}{1-\Theta}\right) \qquad (2)$$

The second is the Fowler−Guggenheim equation for localized adsorption:

$$P = \frac{\Theta}{1-\Theta} K_o^{\ loc} \exp\left(-\frac{U}{RT} - k_1^{loc}\Theta\right) \qquad (3)$$

It should be noted that both K_0 and k_1 constants in the above equations affect the final distribution function. The value of K_0 has a slight impact on the resulting distribution function. It only translates the adsorptive energy scale of the calculated distribution function. While the second parameter k_1 results in a flattening of the curve when the lateral interaction is overestimated and narrow peaks when the lateral interaction is underestimated.[13] Although both K_0 and k_1 constants are not known a priori, however, some estimates can be found in the literature.[27−29] In this work we accept the following theoretical equations for K_0 and k_1^{mob} [27]

$$K_0^{\ mob} = \left(\frac{2\pi m k T}{h^2}\right)^{1/2} \cdot \frac{kT}{\beta} \qquad (4)$$

$$k_1^{\ mob} = \frac{2\alpha}{\beta k T} \qquad (5)$$

where α and β are two-dimensional analogues of the van der Waals constants a and b. The final values used in the calculations are $K_0 = 1.368 \times 10^6$ Torr (or $K_0 = 1.8 \times 10^3$ if P_0 is included in this constant) and $k_1^{mob} = 5.622$.

For all calculations absolute prior knowledge (nonnegative solution) was used. The nonnegativity constraint is known to be very powerful for eliminating the oscillating solutions. Another strategy, the principle of parsimony, was used to obtain the simplest solution (smoothest), that is, the solution that has the least details. While this solution may not have all the detail of the true solution, the detail that it does have is necessary to fit the data. The regularization parameter was chosen by the CONTIN program on the basis of PROB1 TO REJECT criteria. Details of this method may be found in the original work of Provencher.[16] However, the chosen-by-CONTIN solution was finally compared with all possible solutions to check whether it is consistent with all other knowledge. CONTIN also computes the covariance matrix of the solution under the assumptions that the regularizor is not biasing the solution and that there are enough parameters to represent the solution adequately. Therefore, as the regularization parameter is very large, the error bars ($(\Sigma)^{1/2}$ is plotted as error bars) lose all meaning and approach zero.

3. Results and Discussion

3.1. Simulated Isotherms. Resolving Power and Validating Method. First, the CONTIN program was tested for calculation of the AED using simulated isotherms. Since the true distribution in this case is well-known, it is possible to analyze the effect of the error inherent in the input isotherm, the range of relative pressure used for calculation, and the number of data points on the isotherm on the obtained distribution function. Figure 2 shows AEDs calculated from the 50-point isotherm simulated over a wide range of P/P_0 values (Table 1, data set 1). The dotted vertical lines show the energy range calculated using the CA method for the HdB equation. The distributions were calculated over a slightly wider range than that estimated by the CA. It follows from this figure that CONTIN provides perfect recovery of the original distribution if sufficient information is inherent in the input data. In the case of a large data set calculated over a wide range of relative pressures, the level of error does not affect the resulting distribution up to 10%. The only noticeable change in the calculated

(21) Isirikyan, A. A.; Kiselev, A. V. *J. Phys. Chem.* **1961**, *65*, 601.
(22) Fernandez-Colinas, J.; Denoyel, R.; Grillet, Y.; Rouquerol, F.; Rouquerol, J. *Langmuir* **1989**, *5*, 1205.
(23) Rodriguez-Reinoso, F.; Martin-Martinez, J. M.; Prado-Burguete, C. *J. Phys. Chem.* **1987**, *91*, 515.
(24) Carrot, P. J. M.; Roberts, R. A.; Sing, K. S. W. *Carbon* **1987**, *25*, 769.
(25) Kaneko, K.; Ishii, C.; Ruike, M.; Kuwabara, H. *Carbon* **1992**, *30*, 1075.
(26) Puziy, A. M.; Matynia, T.; Gawdzik, B.; Poddubnaya, O. P. *Adsorpt. Sci. Technol.* **1998**, *16*, No 3, 225.
(27) House, W. A.; Jaycock, M. J. *Colloid Polym. Sci.* **1978**, *256*, 52.
(28) Jaroniec, M.; Sokolowski, S.; Rudzinski, W. *Z. Phys. Chem. (Leipzig)* **1977**, *258*, 818.
(29) Adamson, A. W. *Physical Chemistry of Surfaces*; Wiley-Interscience Publ., John Wiley and Sons: New York, 1976.

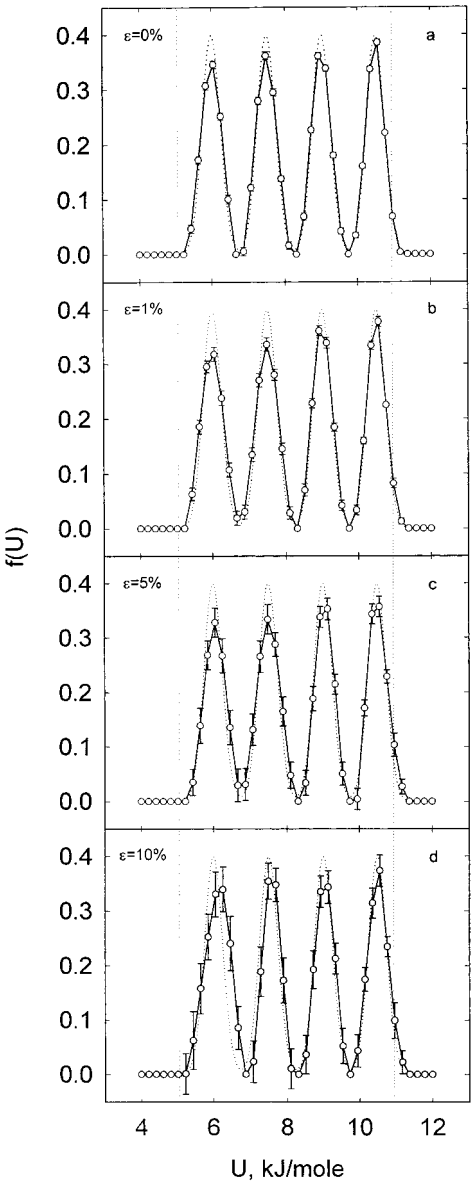

Figure 2. Effect of error level on the adsorption energy distribution calculated from simulated isotherm data set 1.

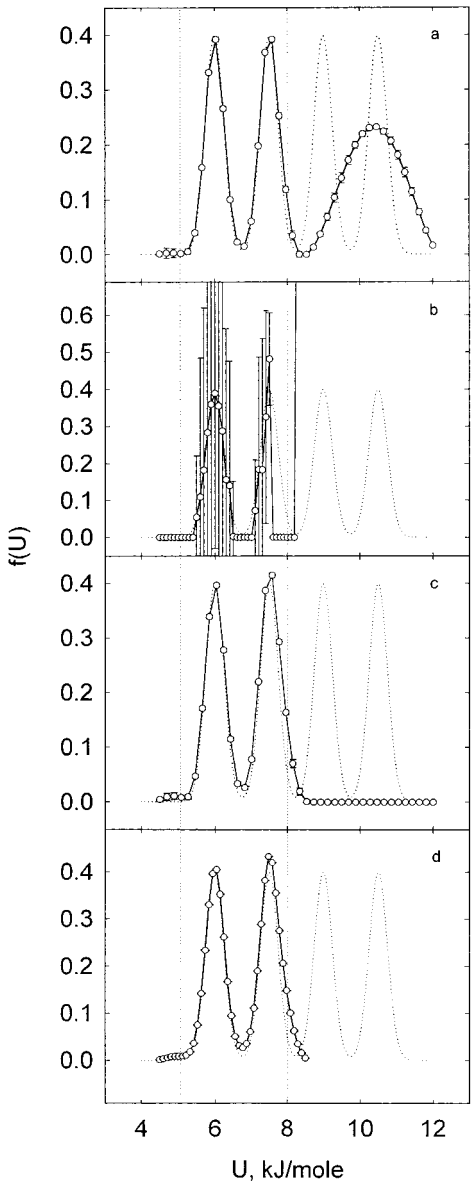

Figure 3. Effect of the constant background term and the calculated energy range on the adsorption energy distribution from simulated isotherm data set 2. Calculations without (a and b), and with the constant background term (c and d).

distribution is the increasing of error bars, thus indicating the increasing of the error level in the adsorption isotherm.

Figure 3 shows AEDs calculated from the 50-point isotherm simulated for a narrow pressure range (Table 1, data set 2). In this case the energy range calculated by the CA method covers only two low-energy peaks. Calculating the distribution function over an energy range considerably wider than the CA region gives bad recovery of the two high-energy peaks that lie outside the CA region (Figure 3a): they are represented as one peak. However, the two low-energy peaks at 6.0 and 7.5 kJ/mol were recovered quite well. From this analysis it is apparent that the adsorption isotherm contains (i) full information about the distribution within the CA range and (ii) enough information only about the existence of peaks beyond the CA region, but not enough information about the details of the distribution (number of peaks, location, area, etc.). Seemingly, the solution for this problem could be achieved by merely narrowing the calculated range of the AED to the CA energy range; however, Figure 3b shows that in this case the distribution is inadequate with enormously increased error bars. What this means is that the data require high-energy peaks for correct description of the isotherm. CONTIN offers a possibility to introduce a constant background term in the calculation and thus to compensate the influence of peaks which are located beyond the calculated region. Figure 3c and d shows the results of the calculation of the AED using a constant background term. The level of the calculated background is equal to the total area of the two high-energy peaks. Both narrow and wide energy range calculations perfectly revealed two peaks situated within the CA region (Figure 3c and d) and did not show any peaks in the higher energy range. By comparing the AEDs calculated with and without a constant background term it is possible to reveal the existence of peaks outside the CA region that cannot be reliably calculated. Hence, in a further analysis we will restrict calculations to the CA region or a slightly wider region. Figure 4 shows the effect of the error level in the input isotherm on the AEDs calculated from data set 2 using a constant background. Both low-energy peaks recovered quite well up to the error level 5%, and even at 10% error the distribution, while strongly smoothed, still shows two peaks at the right positions. It is evident from

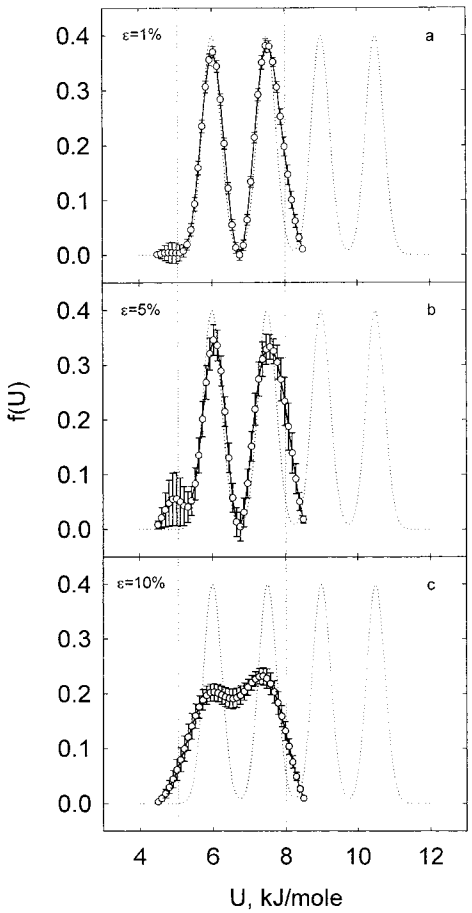

Figure 4. Effect of error level on the adsorption energy distribution calculated from simulated isotherm data set 2.

this figure that for data sets with sufficiently large amount of data points it is possible to obtain reliable information about the distribution within the CA region even when data contain a high level of noise.

Figure 5 shows the effect of error on the distribution function when an isotherm with a small amount of data points is used (Table 1, data set 3). The recovery of the original distribution is quite good for error levels up to 1%. Although the distribution function obtained for a higher error level (5%) becomes smoothed, however, it still may be recognized as satisfactory because all four peaks are located at the right positions. And only error as high as 10% greatly destroyed the solution for the two low-energy peaks, while the two high-energy peaks recovered quite satisfactorily. Notice the increased error bars for the low-energy region. This means that the solution is better defined by the available data in the high-energy range than by that in the low-energy range.

The most severe situation occurs in calculation of synthetic data set 4, where there is a small amount of data points over a narrow pressure range. Figure 6 shows that the original distribution may be recovered well up to the error level 5%. 10% error gives very a flattened distribution with two noticeable components at positions of the true solution. However, it should be noted that extra peaks may appear in this case.

The crucial question that arises after the calculation of the distribution function has been obtain is whether the model used fits the data or not. The estimation or validation of the model can be done on the basis of analysis of the residuals of the fit to the data. If the residuals of the fit are of a reasonable level compared to experimental

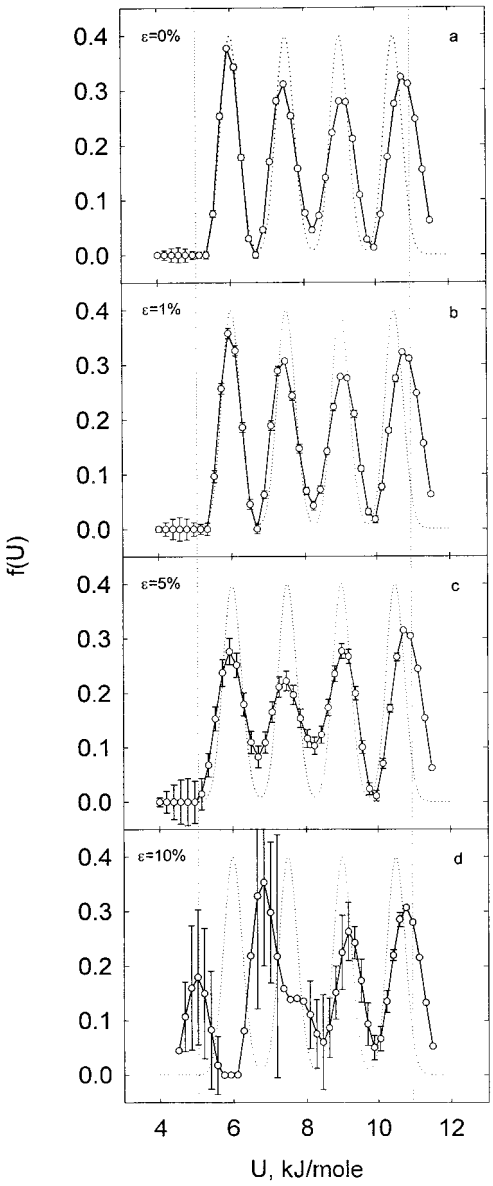

Figure 5. Effect of error level on the adsorption energy distribution calculated from simulated isotherm data set 3.

error and they are of a random nature, the model is adequate. Large deviations, that display trends and other departures from randomness, are strong grounds for rejecting or at least amending the model. For this purpose CONTIN calculates the objective parameter PRUNS, number of runs (a sequence of residuals of equal sign) in the residual, characterizing the randomness of the scatter in the errors of the fit to the data.[30,31] Unfortunately, these parameters work well only for a large data set (≈100). On frequent occasions experimental isotherms do not meet these criteria. Also PRUNS cannot detect a systematic trend in the magnitudes of the residuals; therefore, the visual observation of the error plot provides a useful guide for recognition of a systematic lack of fit or outliers.

Figure 7 shows the number of runs, PRUNS, calculated for simulated data set 1 with 1% error (Table 1) using the mobile adsorption model (HdB) and the localized adsorption model (FG). Large values (>0.1) are indications of well scattered residuals while small values are warning

(30) Provencher, S. W. *J. Chem. Phys.* **1976**, *64*, 2772.
(31) Bard, Y. *Nonlinear Parameter Estimation*; Academic Press: New York, 1974.

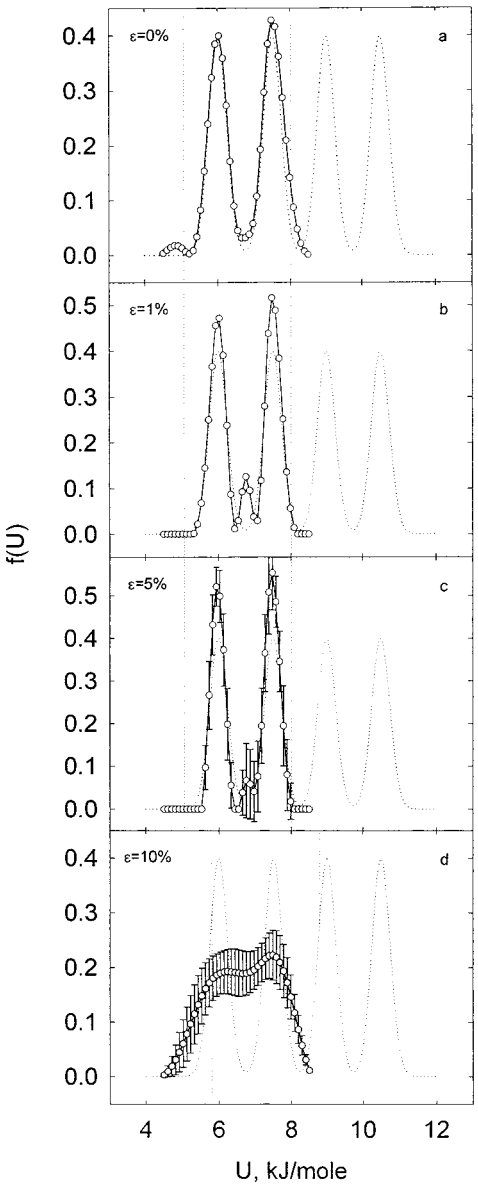

Figure 6. Effect of error level on the adsorption energy distribution calculated from simulated isotherm data set 4.

that they are nonrandom. Although it follows from this figure that for the mobile adsorption model only small values of the lateral interaction constant k_1^{mob} are below the level of PRUNS = 0.1 (shown as dotted line in Figure 7), however, a sharp maximum corresponding to the true value $k_1^{mob} = 5.622$ used for simulation is clearly seen. The same trend is observed when the localized adsorption model is used: only very low values of k_1^{loc} gives PRUNS below 0.1. The existence of an extremum on the curve gives us grounds to expect that this will be a help in estimating the model and its optimal parameters in the case of experimental data. It also follows from this figure that the mobile adsorption model can be fitted well with the localized adsorption equation if the proper lateral interaction constant is used. This fact shows that a good fit does not prove the model; it merely establishes that the model cannot be disproved by the data.

3.2. Graphitized Carbon Black. Validating the Model. Nitrogen adsorption on a classical homogeneous surface, graphitized carbon black Sterling FT 2800[21] furnishes a unique opportunity to estimate the validity of the adsorption model. Adsorption of nitrogen on this carbon black was carefully analyzed by de Boer and co-

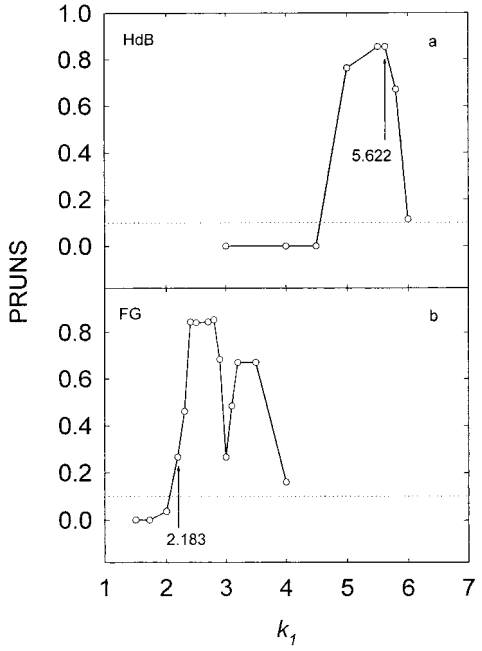

Figure 7. Effect of the lateral interaction constant in the HdB equation (a) and the FG equation (b) on the number of runs, PRUNS, for simulated isotherm data set 1 with 1% error.

workers,[32] and it was found that adsorption of nitrogen on graphitized carbon black is more mobile then localized. However, the model of localized adsorption is also often applied for analysis of nitrogen adsorption on microporous carbon adsorbents.[33,34] Considering that these models are widely used, we will compare mobile and localized adsorption models for the description of nitrogen adsorption on a homogeneous surface with the help of the method outlined in the previous section.

A relatively large number of available experimental points allows for analysis of scatter in the residuals of the fit. Figure 8 shows the number of runs, PRUNS, calculated for nitrogen adsorption on graphitized carbon black Sterling FT using the mobile adsorption model (HdB) and the localized adsorption model (FG). It is clearly seen from this figure that both curves display a distinct maximum. For the mobile adsorption model this maximum is very close to the theoretical value 5.622 derived from two-dimensional gas properties (eq 5). However, for the localized adsorption model the maximum appears at $k_1^{loc} = 3$, a value larger than 2.183, derived as one-fourth of the heat of vaporization of nitrogen at the boiling point.[27] It should be noted that the parameter PRUNS for both values of the lateral interaction constant ($k_1^{mob} = 3.648$ and $k_1^{loc} = 1.725$) obtained using the same data set in ref 32 is are below 0.1 and should be regarded as unsatisfactory. The error plot (Figure 9) can visualize the bias in the residuals of the fit for the mobile adsorption model. The residuals at $k_1^{mob} = 3-4$ are very correlated, indicating that the model with this value of the lateral interaction constant is inadequate. When a larger value of the lateral interaction constant is used, the residuals become well scattered and the standard deviation is decreased, approaching a minimum for $k_1^{mob} = 5.5$. The same trend is observed while using FG localized adsorption (Figure 10). The above results show that both models can fit well the

(32) *Physical And Chemical Aspects Of Adsorbents And Catalysts*; Linsen, B. G., Ed.; Academic Press: London, New York, 1970.
(33) Choma, J.; Jaroniec, M. *Langmuir* **1997**, *13*, 1026.
(34) Jagiello, J.; Bandosz, T. J.; Schwarz, J. A. *Langmuir* **1997**, *13*, 1010.

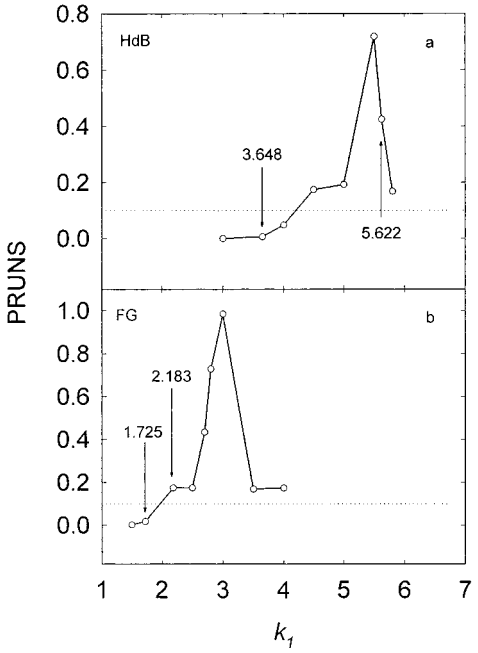

Figure 8. Effect of the lateral interaction constant in the HdB equation (a) and FG equation (b) on the number of runs, PRUNS, for nitrogen adsorption on graphitized carbon black Sterling FT 2800.[21]

nitrogen adsorption on graphitized carbon black if a proper lateral interaction constant is used. However, to obtain a good fit in the case of the localized adsorption model, it is necessary to use a high value of the lateral interaction constant that cannot be theoretically justified for this adsorption system. This provides reason enough to prefer the mobile adsorption model with the lateral interaction constant close to 5.5. Therefore, for further analysis of heterogeneity we will use the Hill−de Boer equation with lateral interaction derived from two-dimensional gas properties $k_1^{mob} = 5.622$.

The adsorption energy distribution for graphitized carbon black Sterling FT[21] calculated using the mobile adsorption model is presented in Figure 11. The distribution is dominated by one sharp peak at 8.8 kJ/mol, which can obviously be attributed to adsorbent−adsorbate interaction on the basal plane of graphite (Figure 11a). The existence of another three peaks at 4.9, 6.6, and 10.3 kJ/mol indicates other types of interaction between nitrogen and the carbon surface. The first of these peaks is due to multilayer adsorption while the other two may be attributed to various imperfections in the structure of the carbon surface, including surface impurities, surface defect structure, edges, steps or different exposed crystal faces. However, their intensities are very low. Calculation with and without background gives the same distribution function indicating that all peaks are covered by available data and that no other peaks are necessary for adequate description of the isotherm. The regularization parameter estimated by CONTIN was low ($= 5 \times 10^{-4}$), indicating the good quality of the experimental data. However, the distribution shows more peaks, as might be expected for a homogeneous surface. This raises the question of whether all peaks on the distribution are necessary for accurate description of the isotherm. A peak-constrained analysis provided by CONTIN is very useful for revealing the artifacts in the calculated distribution. During the peak-constrained analysis, CONTIN tries to find the solution with smallest number of peaks that is consistent with the data. The results of one-peak and two-peak constrained analysis show that constraints have forced

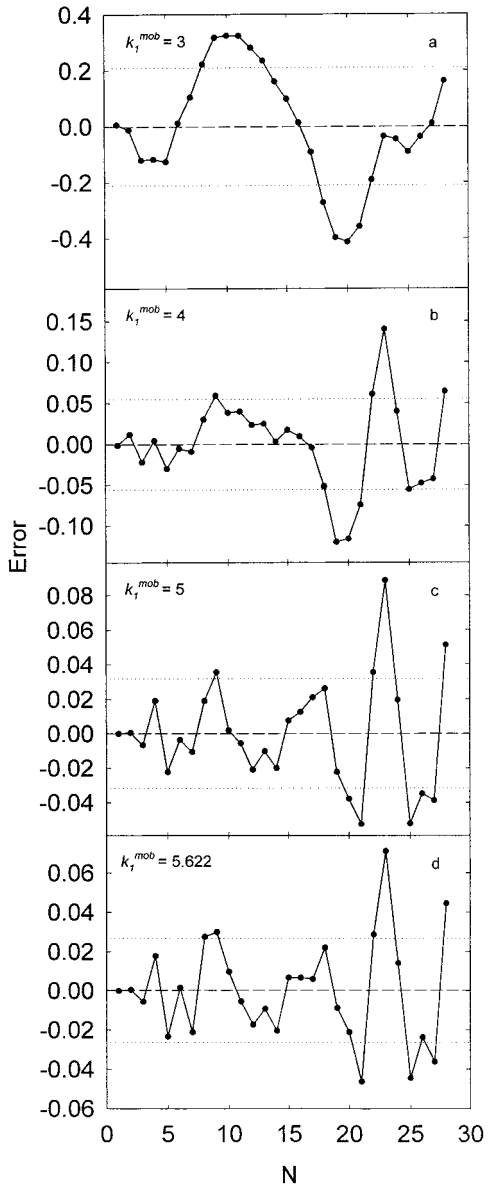

Figure 9. Error plot of the CONTIN fit to nitrogen adsorption on graphitized carbon black Sterling FT 2800[21] using the HdB local isotherm with different lateral interaction constants. Dashed lines show the mean, and dotted lines show the standard deviation.

the solutions to have one peak (Figure 11b) and two peaks (Figure 11c). However, the peaks have been replaced with flat spots or plateau at both sides of the peaks. During the peak-constrained analysis it was not possible to cleanly eliminate these flat spots by increasing the regularization parameter even at large values. This allows us to say with more confidence that the data require all original peaks, since solutions with fewer peaks that were consistent with the data could not be found.

3.3. Standard Nitrogen Adsorption Data. Figure 12 shows adsorption energy distributions calculated from nitrogen adsorption data proposed as the standard isotherm for use in the α_s method.[22−25] Although the distributions are different, however, they show common peaks at 4.9, 6.8, and 8.8 kJ/mol characteristic of graphitized carbon black Sterling FT. The first peak is obviously attributed to the beginning of polymolecular adsorption. The peak at 8.8 kJ/mol should be attributed to interaction between nitrogen molecule and the basal plane of the graphitic structure while the peak at 6.8 is

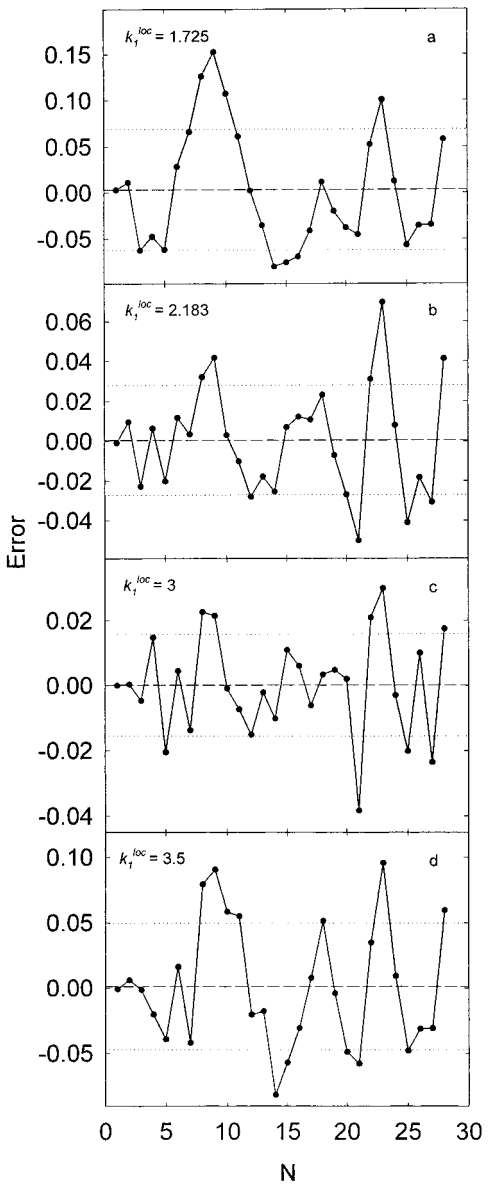

Figure 10. Error plot of the CONTIN fit to nitrogen adsorption on graphitized carbon black Sterling FT 2800[21] using the FG local isotherm with different lateral interaction constants. Dashed lines show the mean, and dotted lines show the standard deviation.

due to the presence of other crystallographic planes exposed to the surface. The peak at 5.9 kJ/mol occurring in the form of a sharp peak or a shoulder in all distributions for ungraphitized carbon materials is most pronounced for carbon A (Figure 12b). Probably this peak is attributed to oxygen-containing surface groups, since this carbon was prepared from olive stones, a lignocellulosic material that contains a considerable amount of oxygen. The presence of this peak is the reason for the significant difference in the shape of the isotherms for carbon A and the standard isotherm at low relative pressures, as discussed in ref 24. NPC carbon (Figure 12d) shows the most heterogeneous surface among the investigated carbons with the new peaks at 7.7 and 9.6 kJ/mol. The high-energy peak at 9.6 kJ/mol may be attributed to the presence of some microporosity, while the nature of peak at 7.7 could be discussed on the basis of the known processing history of this carbon. The low-pressure range available for the isotherms for carbon A and standard nonporous carbon (Figure 12b and c) restricts calculation

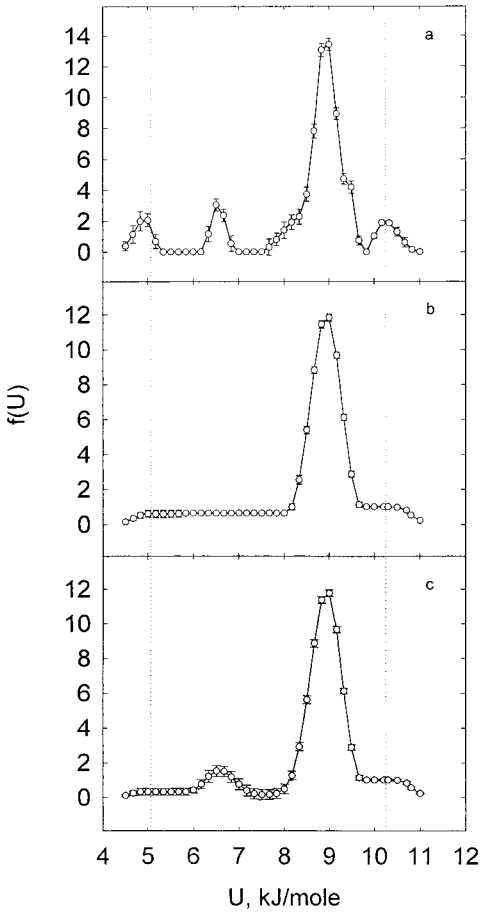

Figure 11. Adsorption energy distribution for graphitized carbon black Sterling FT 2800:[21] (a) chosen solution; (b) one-peak-constrained solution; (c) two-peak-constrained solution.

of the AED to energies lower thant that of the peak attributable to the interaction of nitrogen with the graphitic structure of carbon. The high level of background (141% for carbon A and 42% for standard nonporous carbon) calculated for these two carbons is indicative of the existing peaks with energies higher than 7 kJ/mol, while for Vulcan and NPC carbon the background was low (4%), suggesting that all peaks are revealed.

3.4. Synthetic Carbons. Figure 13 shows adsorption energy distributions for the copolymer BM-ST and the synthetic carbons C1, C2, and C3 obtained using different carbonization procedures. Due to the small adsorption capacity at low pressures, the isotherms for the parent copolymer BM-ST and the synthetic carbons after chemical vapor deposition (carbons C2 and C3) were available only for relatively high pressures. All adsorbents, including the parent polymer, show low-energy peaks located at 4.5−5.0 kJ/mol which may be attributed to multilayer adsorption. In addition to this peak, the distribution for the parent copolymer BM-ST shows two others peaks at 5.4 and 6.6 kJ/mol. The reason for these peaks may be the interaction of the nitrogen molecule with different surface groups of the polymer. The distribution covers only half of the existing peaks (the background equals 110% of the total distribution). The distribution for carbon C1 obtained by carbonization in an inert atmosphere shows four peaks at 4.6, 5.8, 7.3, and 10.3. The positions of the first three peaks are similar to those obtained for reference carbons (Figure 12), while the high-energy peak may be attribute to the presence of micropores. The background term obtained for this distribution equals 55% of the total distribution, indicating that there exist peaks at higher

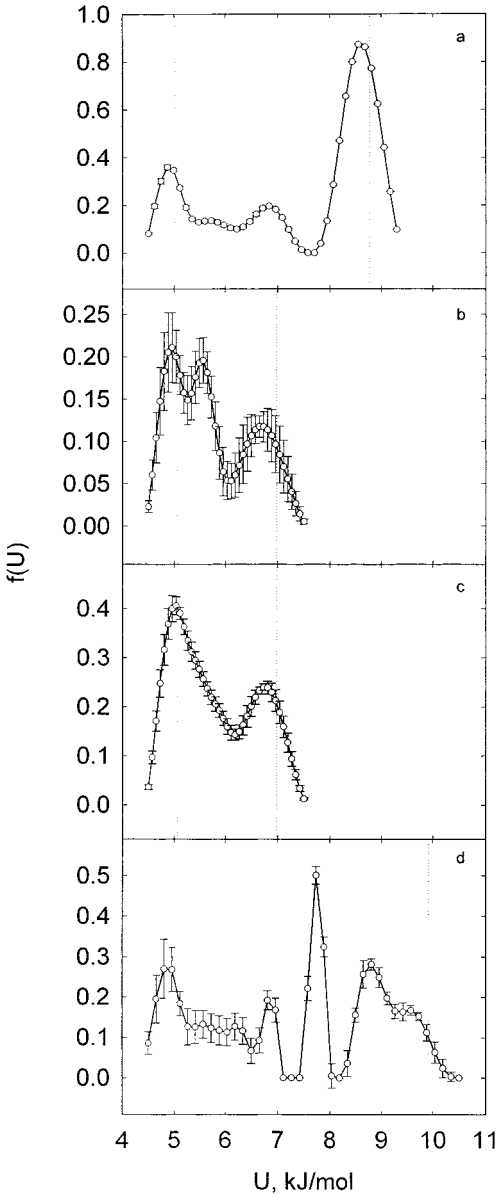

Figure 12. Adsorption energy distributions for untreated Vulcan carbon black[22] (a), carbon A[23] (b), and for nonporous carbon[24] (c).

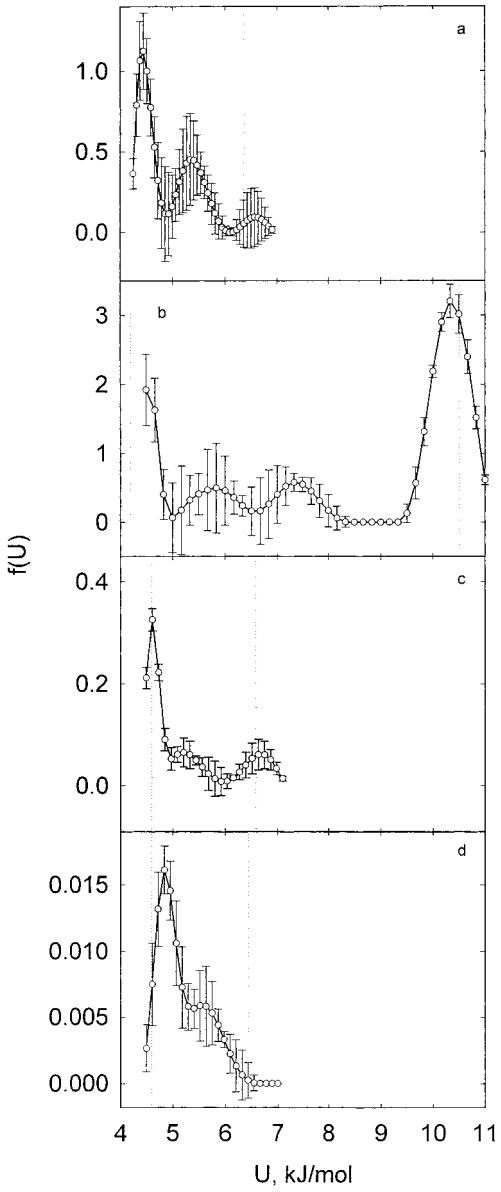

Figure 13. Adsorption energy distributions for the porous polyimide copolymer BM-ST (a) and synthetic carbons C1 (b), C2 (c), and C3 (d).

energies, or at least that the peak continues to higher values. It should be noted that there is no peak corresponding to the interaction of nitrogen with the basal plane of graphite (8.8 kJ/mol). The reason is that carbon C1 was obtained at relatively low temperature (600 °C) when the graphitic structure is not formed. The deposition of pyrolitic carbon (CVD in CH_4 atmosphere) on sample C1 results in decreasing the intensity of the distribution (decreasing the total area of peaks). Longer exposure to a CH_4 atmosphere at high temperature (sample C2) causes further decreasing of the intensity of the distribution. Despite the fact that the high-energy region is available only for carbon C1, it is possible to estimate the relative area of peaks higher than say 7 kJ/mol. The fraction of the distribution with peaks higher than 7 kJ/mol equals 48, 29, and 8% for samples C1, C2, and C3, respectively. These values show progressive deposition of carbon in micropores.

4. Conclusions

The analysis of an adsorption isotherm using the CONTIN method for inverting noisy linear operators appears to be a powerful tool for investigating the heterogeneity of the adsorbent. This method was used to calculate the adsorption distribution function from both simulated and experimental adsorption isotherms. Simulated isotherms allowed us to estimate the resolving power of the method and the influence of errors on the distribution function, while experimental isotherms enabled us to validate the adsorption model and its parameters. It was shown that calculation within condensation approximation region gives perfect recovery of the original distribution if sufficient information is inherent in the input data, that is, in the case of a large data set over a wide range of relative pressures. When only a window of data is available on the adsorption isotherm, it is possible to calculate the distribution restricted to the CA region. The influence of peaks outside the CA region may be eliminated by introducing the constant background term in the calculation. The level of error does not affect the resulting distribution up to 10% in the case of a large data set and up to 5% in the case of a small data set.

On the basis of the analysis of a sequence of residuals of equal sign, characterizing the randomness of the scatter

in the errors of the fit to the data, it was possible to establish the true parameter of the lateral interaction constant. This approach applied to experimental data has led to the value $k_1^{mob} = 5.5-5.6$ for the HdB mobile adsorption model and $k_1^{loc} = 3$ for the FG localized adsorption model. On the basis of the fact that the optimal value of k_1^{mob} is closer to the theoretical value, the mobile adsorption model is preferred.

The CONTIN method applied to graphitized carbon black revealed four peaks on the adsorption energy distribution function. The peak-constrained analysis allowed us to confirm the existence of all original peaks.

The distributions calculated from the standard nitrogen adsorption data revealed that although reference carbons are heterogeneous in different ways, they show common peaks at 4.9, 6.8 and 8.8 kJ/mol characteristic of graphitized carbon black Sterling FT.

Analysis of the heterogeneity of synthetic carbons revealed the changes in the AEDs that occur during CVD from methane.

Acknowledgment. Dr. S. W. Provencher is gratefully acknowledged for help in learning CONTIN.

LA981369T